Torque Density of Radial, Axial and Transverse Flux Permanent Magnet Machine Topologies

Jenni Pippuri, Aino Manninen, Janne Keränen, and Kari Tammi

VTT Technical Research Centre of Finland, 02044 Espoo, Finland

Torque density of radial, axial and transverse flux machine topologies is investigated. A 10-kW, 200-rpm motor is chosen as a test case. Radial and axial flux motors that fulfill the key specifications of the selected test case are designed employing in-house analytical dimensioning tools and MATLAB genetic multi-objective optimization. Rather simple numerical approach is taken to study the transverse flux motor. A 20-pole-pair radial flux motor is found to outperform its axial and transverse flux counterparts in terms of torque density.

***Index Terms*—AC machines, electromagnetic analysis, machine designing, torque density.**

I. Introduction

MODERN electric machines and drives are facing rather versatile requirements. On one hand, energy efficiency has perhaps never been higher on the agenda; in the field of electric machinery more energy efficient practices are enforced by standardization. On the other hand, the areas of application of electric machines and drives are ever wider. Meeting the requirements of the latter trend necessitates developing solutions beyond conventional ones. For example, an electric drive of a hybrid or electric vehicle must not only be energy efficient but also as compact as possible [1]. In this work, the compactness of three different machine topologies is assessed.

Obviously, at least a fairly compact design for any electric machine can be attained through efficient cooling. The more effective the cooling is, the higher electric and magnetic loadings can be allowed and consequently the more compact design attained. Second, the size of a machine depends greatly on its operation speed. While the power is kept constant, the torque decreases inversely proportionally with increasing speed and as a result, the mass and volume of the machine decrease.

Besides cooling and operation speed, the basic topology of a machine determines its size to some extent. The concept of topology encompasses various aspects. For instance, does the machine have a separate magnetization winding or is it magnetized through the armature winding.

This work investigates the torque density of radial, axial and transverse flux permanent magnet machines in a certain power class. The concentration is on permanent magnet machines for the reason of their inherently high torque density [2].

II. Methods

A. Example Motor Specification

This work is carried out using a 10-kW, 200-rpm three-phase motor as a test case. Such a motor could be fit, for instance, for small scale propulsion. The RMS value of the phase voltage of the motor is set to be 230 V. As the characteristics of transverse flux machines improve with increasing number of poles, they are typically best fit for low speed applications [3], [4]. This matter guided the selection of the speed range of this study.

Manuscript received November 10, 2012; revised December 21, 2012; accepted December 21, 2012. Date of current version May 07, 2013. Corresponding author: J. Pippuri (e-mail: jenni.pippuri@vtt.fi).

Color versions of one or more of the figures in this paper are available online at http://ieeexplore.ieee.org.

Digital Object Identifier 10.1109/TMAG.2013.2238520

The magnets of the machines are mounted on the rotor surface and each of them covers 70 percent of a pole pitch. The radial flux designs are of the conventional inner rotor type, the axial flux designs have a single rotor, single stator construction and transverse flux machine has a U- and I-core stator layout with an inner rotor of two separate yokes [3]. Many other configurations exist, too, [4]–[6], but now, for the sake of simplicity, the concentration is on the basic ones. Furthermore, the radial and axial flux machines are designed to have a simple single layer lap wingdings. The armature winding of the transverse flux machine is a ring-shaped one.

B. Analytical Design and Optimization of Radial and Axial Flux Machines

The radial and axial flux machines are designed using analytical in-house tools that are implemented in MATLAB. Both of these tools are founded on the same basic principles [7], [8]. First, the design task is initialized by setting the main characteristics (output power, speed, supply etc.). Second, the main dimensions that are the rotor outer diameter and rotor length for radial flux machines and stator outer and inner diameter for axial flux machines are solved based on the tangential stress or force density.

When the main dimensions are known, the armature winding arrangement is chosen and detailed dimensions of conductors and cores are worked out based on the allowed electric and magnetic loadings. The magnetic circuits of the machines are represented with simple no-load reluctance networks [8], [9]. The reluctance network of the axial flux machine is adapted from that presented in [8].

After the electromagnetic designing has been completed, the machine characteristics, efficiency, losses etc., are solved and finally, the feasibility of the design that is obtained is assessed by means of thermal analysis. The thermal network of radial flux machines has been discussed in detail in [8], [10]. The thermal network of axial flux machines consists of 66 elements and has been developed using the general cylindrical component that has been presented in [11].

For finding the most appropriate designs for the task at hand, the analytical design tools are utilized in combined with the MATLAB optimization routines.

1) Optimization: An electric machine can be optimized from various aspects: e.g. efficiency, mass, torque density, and material costs. Here, the principal aim is to maximize torque density, but this cannot mean that the efficiency is poor. Thus, both of these quantities are chosen to be optimized by multi-objective optimization, and their possible contradictions are analyzed. However, as the torque is kept fixed, instead of

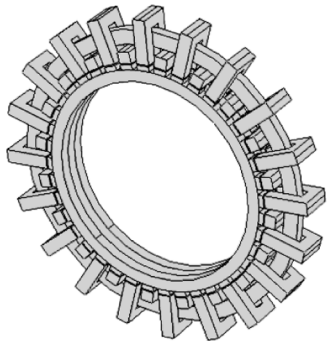

Fig. 1. A single phase unit of a transverse flux machine.

maximizing the torque density, the total volume of the motor is minimized.

In multi-objective optimization, there is no single solution that simultaneously optimizes both objectives, but one gets a set of optimal solutions, called a Pareto optimal front. The Pareto optimal solutions are such that, when trying to improve an objective further, other objectives suffer as a result.

The NSGA-II genetic algorithm [12] from the Global Optimization Toolbox of MATLAB was used. As the multi-objective genetic algorithm in MATLAB does not support mixed integer optimization, the optimization routine had to be run separately for different pole pair numbers.

C. Finite Element Analysis of Transverse Flux Machines

The complicated flux patterns of transverse flux machine are difficult to capture by analytical means. Research on the topic, however, is rather active and different solutions for representing the leakage flux paths have been presented [13]. Here, instead of analytical approach, a simple three-dimensional (3-D) numerical analysis is used for finding the transverse flux machine design for the comparison purpose.

A three-phase transverse flux machine can be constructed from three identical single phase units, such as the one given in Fig. 1. Obviously, for being able to create 3-D model of a machine, initial estimates for its dimensions must be found by some means [2], [14]. First, the radial height, h_{PM}, of the magnets is solved from [2]

$$h_{\mathrm{PM}} = \frac{\mu_{\mathrm{PM}}\delta}{\frac{B_{\mathrm{r}}}{B_{\mathrm{p}\delta}} - 1} \tag{1.1}$$

in which μ_{PM} denotes the relative permeability of the magnets, B_{r} their remanent flux density, $B_{\mathrm{p}\delta}$ the peak value of air gap flux density and δ the air gap length. The peak value of flux density is set to be 0.8 T, the air gap length and the remanent flux density of the magnet grade being 2 mm and 0.9962 T, respectively.

While the magnet height and air gap length have been settled, the value of linear current density for the modeled geometry is solved from

$$A = \frac{\sqrt{2}\sigma_{F\tan}}{B_{\mathrm{p}\delta}\alpha_{\mathrm{PM}}} \tag{1.2}$$

in which $\sigma_{F\tan}$ denotes the tangential stress and α_{PM} the ratio of circumferential magnet width to the circumferential pole width, i.e. here 0.7. This value is later employed to estimate the total current density in the phase winding from the dimensions of the stator. Estimates for the rotor outer diameter and rotor length are defined first based on the tangential stress acting on the rotor. The dimensions of stator U- and I-cores and rotor cores depend on those of permanent magnets as shown in Table I, in which w_{tUc}, w_{yUc}, w_{Ic}, and w_{PM} denote the circumferential widths of the stator U-core teeth, the stator U-core yoke, stator I-cores, and permanent magnets, respectively. Furthermore, l_{tUc} denotes the axial length of the stator U-core teeth, h_{yUc} the height of the stator U-core yokes, h_{yr} the height of the rotor cores, h_{Ic} the height of the stator I-cores and l_{PM} the axial length of the permanent magnets. The axial length of the stator phase coil is adjusted according to the dimensions of the stator U-cores. The slot height is then defined based on the allowed current density in the slot. Here, the current density in the stator coil should not exceed 3 $\mathrm{A/mm^2}$. A rather low limit for the current density is given in order to ensure that the magnets do not overheat.

TABLE I
DEPENDENCIES BETWEEN DIMENSIONS OF STATOR U- AND I-CORES, ROTOR CORES AND PERMANENT MAGNETS

$w_{\mathrm{tUc}} = w_{\mathrm{yUc}} = w_{\mathrm{Ic}} = w_{\mathrm{PM}}$
$l_{\mathrm{tUc}} = h_{\mathrm{yUc}} = h_{\mathrm{yr}} = h_{\mathrm{Ic}} = l_{\mathrm{PM}}$

After the initial estimates of the dimensions are known, a multi-static FEM solution of the magnetic field $\boldsymbol{B}$, for a rotor positions that cover one pole pair, is executed. Magnetic vector potential $\boldsymbol{A}$, such that $\boldsymbol{B} = \nabla \times \boldsymbol{A}$, is solved from

$$\nabla \times \nu \nabla \times \boldsymbol{A} = \left\{ \begin{array}{cc} 0 & \text{air, core} \\ \nabla \times \boldsymbol{H}_{\mathrm{c}} & \text{permanent magnets} \\ \boldsymbol{J} & \text{stator winding} \end{array} \right\} \tag{1.3}$$

in which ν denotes reluctivity, $\boldsymbol{H}_{\mathrm{c}}$ coercive field strength, and $\boldsymbol{J}$ current density. The torque production capability of the machine is solved from the field solution. If needed, the dimensions are adjusted and the multi-static analysis repeated until the target torque value is reached.

Comsol Multiphysics is used to compute the magnetic fields [15]. The approach taken to the designing of the transverse flux machine is an approximate one and the optimization and more detailed analysis of this machine type is a topic of further investigations.

III. RESULTS

A comparison between the radial and axial flux designs is presented in the first section. These designs were obtained by looking a maximum torque density with a good efficiency, preferably above 0.92. In the second section, the torque density of 20-pole-pair radial, axial and transverse flux machines is discussed.

The design process of all the machine topologies was carried out keeping the tangential stress constant, its value being 14000 Pa. During the optimization of radial and axial flux machines, the peak magnetic flux density in the air gap, the current density in stator conductors, J_{c}, k_{RF}, i.e. the ratio of axial length to rotor outer diameter, k_{AF}, i.e. the ratio of stator inner diameter to its outer diameter, and air gap length were allowed to vary as tabulated in Table II. Table II summarizes the input parameters that were used for designing the transverse flux machine, too.

Throughout the study, the *total volume* was evaluated from

$$V_{\mathrm{tot}} = \left(\frac{D_{\mathrm{o}}}{2}\right)^2 \pi l_{\mathrm{tot}} \tag{1.4}$$

TABLE II
INITIAL CONDITIONS OF DESIGN AND OPTIMIZATION

	Radial flux	Axial flux	Transverse flux
$B_{p\delta}$ (T)	0.6-0.9		0.8
J_c (A/mm^2)	2.5-6.5		3
δ (mm)	0.5-6		2
k_{RF} (-)	0.4-3	-	-
k_{AF} (-)	-	0.59-0.75	-

TABLE III
D_o AND l_{tot} FOR THE DIFFERENT TOPOLOGIES

Topology	D_o	l_{tot}
Radial flux	D_{os}	l_c+2·l_{ew}
Axial flux	D_{or}+2·l_{ew}	l_{tot}
Transverse flux	D_{os}	l_{tot}

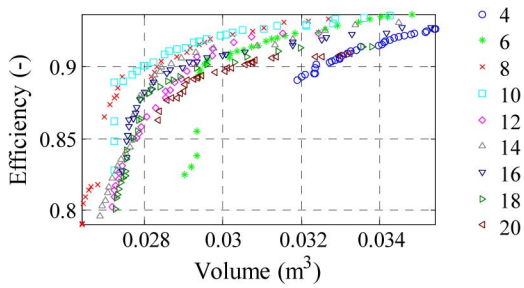

Fig. 2. Pareto optimal fronts of efficiency and *total volume* for radial flux topology. Legend denotes the number of pole pairs in the machine.

in which D_o denotes the outer diameter of the motor, l_{tot} the total axial length of the machine. Definitions of D_o and l_{tot} for the investigated topologies are given in Table III, in which D_{os} denotes the stator outer diameter, D_{or} the rotor outer diameter, l_{ew} the length of end winding, and l_c the core length.

A. Pareto Optimal Fronts of Radial and Axial Flux Topologies

Total-volume versus efficiency Pareto optimal fronts for radial and axial flux machines are shown in Fig. 2 and Fig. 3, respectively. It can be seen from Fig. 2 that if a compact yet sufficiently energy efficient radial flux machine is aimed at, for the given specification, the pole pair number should be between 8 and 10. With lower pole pair numbers, a good efficiency is obtainable but at the expense of *total volume*. If, again, the pole pair number is above 10, the efficiency starts to descend. This is partly due to the increasing supply frequency as the operation speed was kept constant throughout the study.

The fittest axial flux designs in terms of efficiency and size have 10 to 12 pole pairs. As in the case of radial flux designs, it is possible to attain a sufficient efficiency with lower pole pair numbers but not a very compact size. This originates partly from the low supply frequency. In addition, the end windings of the lower-pole-pair designs become lengthy in comparison with those of the higher-pole-pair ones. With a pole pair number 16 and above, the losses in the core of the machine become more dominant due to the increased frequency.

In general, the results shown in Fig. 2 and Fig. 3 support the known fact; increasing the size of a machine is a straightforward approach to improve its efficiency. Therefore, the efficiency and torque density are contradicting qualities.

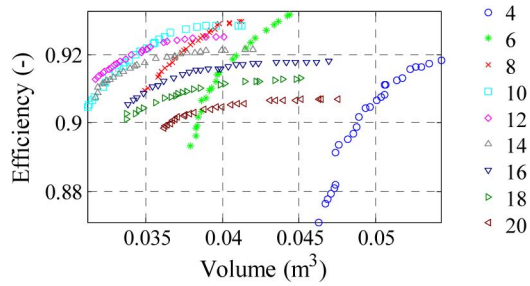

Fig. 3. Pareto optimal fronts of efficiency and *total volume* for axial flux topology. Legend denotes the number of pole pairs in the machine.

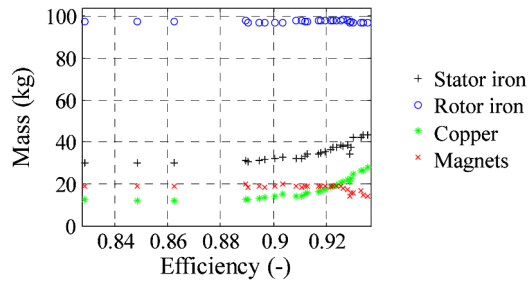

Fig. 4. Masses of active parts of 10-pole-pair radial flux machines in the Pareto optimal front of Fig. 2.

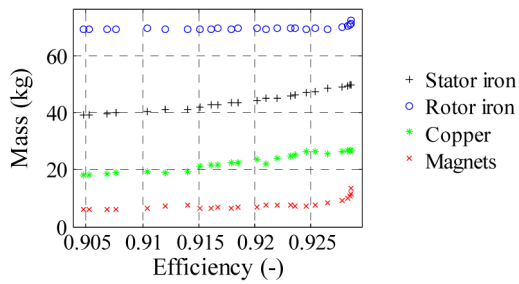

Fig. 5. In the optimized results, masses of active parts of 10-pole-pair axial flux machines.

The masses of the active parts for the radial and axial flux designs, from the Pareto optimal fronts, with a pole pair number 10 are depicted in Fig. 4 and Fig. 5, respectively. Evidently, the amount of copper correlates with the efficiency; the more copper the lower current density and the less resistive losses in the stator windings. A larger winding occupies a greater space that increases the amount of stator iron in the machine, too, as seen from Fig. 4 and Fig. 5. The masses of magnets and rotor iron, instead, are pretty fixed. Clearly, an optimum for the magnet and rotor iron mass is found.

B. Torque Density of 20-Pole-Pair Radial, Axial and Transverse Flux Machine Designs

Next the torque density of 20-pole-pair radial, axial and transverse flux designs is discussed. A high pole pair number was chosen for this comparative study because the characteristics of transverse flux machine improve with increasing number of poles. Based on the previous results, this selection is not in favor of the two other topologies but is justified by the fact that the transverse flux design is not a result of any optimization process.

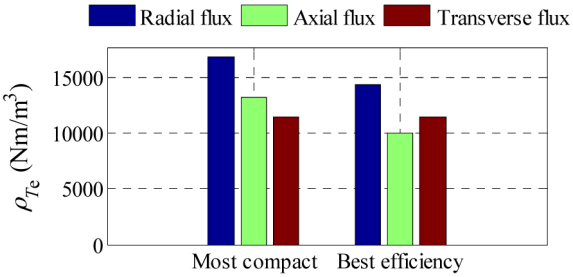

Fig. 6. Torque density of 20-pole-pair, 10-kW, 200-rpm radial, axial and transverse flux machines. Left: the most compact radial and axial flux designs from the Pareto optimal front of Fig. 2 and Fig. 3. Right: The bars of radial and axial flux machine, from the most energy efficient 20-pole-pair-designs.

The torque densities that were evaluated based on the *total volume*, (1.4), are presented in Fig. 6. Both the most compact and most energy efficient 20-pole-pair designs of the radial and axial flux machines were chosen for this comparison from the results that are depicted in Fig. 2 and Fig. 3. It can be seen from Fig. 6 that with the given initial conditions and approach of analysis, the radial flux topology yields the highest torque density. Interestingly, this is the case for even if its size is not the optimum. When comparing the axial and transverse flux machine, the most compact axial flux machine outperforms the transverse flux design whereas for the most efficient axial flux machine the opposite is true.

IV. Discussion and Conclusion

In this work, the properties and particularly the torque density of radial, axial and transverse flux machine topologies was assessed studying a single 10-kW, 200-rpm example machine. The radial and axial machines were designed by means of in-house analytical tools in combined with genetic multi-objective optimization. Only a single transverse flux machine design was considered. The reason for this is that the complex flux patterns of this machine type are rather difficult to capture with analytical reluctance network based approaches and 3-D analysis of magnetic field quickly comes into question. More detailed investigation of the characteristics of transverse flux motors is a topic of further research.

Based on the Pareto optimal fronts it could be concluded that the best radial flux motor designs in terms of efficiency and compactness have a pole pair number from 8 to 10. The axial flux topology was found to perform the best with pole pair numbers 10–12. The lowest pole pair numbers were found to be the least feasible when a compact yet energy efficient solution is sought after. In general, whereas compactness is aimed at the efficiency may become compromised.

The most compact and most efficient 20-pole-pair radial and axial flux designs were extracted from Pareto optimal fronts and compared with the 20-pole-pair transverse flux design. According to the results, the radial flux topology yielded the highest torque density with the given initial conditions and constraints. Based on the previous literature published on the matter, the torque density of the transverse flux machine appears to be low. There is, however, a natural explanation for this result. The transverse flux machine was designed for the same total tangential stress as the other topologies. This was done in order to investigate the differences originating from the orientation of the windings and cores and consequently of the main flux. As higher tangential stresses may typically be allowed in transverse flux machines than in radial and axial ones, the transverse flux design that was presented could be enhanced further in terms of its compactness.

References

[1] C. C. Chan, "The state of the art of electric, hybrid, and fuel cell vehicles," *Proc. IEEE*, vol. 95, pp. 704–718, 2007.
[2] J. F. Gieras and M. Wing, *Permanent Magnet Motor Technology—Design and Applications*. New York: Marcel Dekker, 2002, p. 590.
[3] G. Henneberger and M. Bork, "Development of a new transverse flux motor," *New Topologies for Permanent Magnet Machines (Digest No: 1997/090), IEE Colloquium*, pp. 1/1–1/6, 1997.
[4] Y. G. Guo, J. G. Zhu, P. A. Watterson, and W. Wu, "Development of a PM transverse flux motor with soft magnetic composite core," *IEEE Trans. Energy Convers.*, vol. 21, pp. 426–434, 2006.
[5] A. Parviainen, *Design of Axial-Flux Permanent-Magnet Low-Speed Machines and Performance Comparison Between Radial-Flux And Axial-Flux Machines*. Lappeenranta: Lappeenrannan teknillinen yliopisto, 2005, p. 153.
[6] G. Yang, D. Cheng, H. Zhang, and B. Kou, "Bidirectional crosslinking transverse flux permanent magnet synchronous motor," *IEEE Trans. Magn.*, vol. PP, pp. 1–1, 2012.
[7] J. Pyrhönen, T. Jokinen, and V. Hrabovcová, *Design of Rotating Electrical Machines*. Chichester: Wiley, 2008, p. 512.
[8] A. Manninen, *Evaluation of the Effects of Design Choices on Surface Mounted Permanent Magnet Machines Using an Analytical Dimensioning Tool*, 2012.
[9] T. Heikkilä, *Permanent Magnet Synchronous Motor for Industrial Inverter Applications—Analysis and Design*. Lappeenranta: Lappeenrannan teknillinen korkeakoulu, 2002, p. 109.
[10] J. Lindström, Thermal Model of a Permanent-Magnet Motor for a Hybrid Electric Vehicle Report No. 11R, 1999, 1401-6176.
[11] N. Rostami, M. Feyzi, J. Pyrhönen, A. Parviainen, and M. Niemelä, "Lumped-parameter thermal model for axial flux permanent magnet machines," *IEEE Trans. Magn.*, vol. PP, pp. 1–1, 2012.
[12] B. MathWorks, Matlab vol. 2011, 2011.
[13] K. Lu, P. O. Rasmussen, and E. Ritchie, "Design considerations of permanent magnet transverse flux machines," *IEEE Trans. Magn.* , vol. 47, pp. 2804–2807, 2011.
[14] W. M. Arshad, T. Bäckström, and C. Sadarangani, "Analytical design and analysis procedure for a transverse flux machine," in *Proc. IEEE Int. IEMDC*, 2001, pp. 115–121.
[15] Comsol Web Page, Comsol Web Page for AC/DC Module 2012.